Simulation study of a Ne-like Ti x-ray laser at 32.6 nm driven by femtosecond laser pulses

X. Lu,[1] Y. J. Li,[2] Y. Cang,[1] K. Li,[1] and J. Zhang[1,*]

[1]*Laboratory of Optical Physics, Institute of Physics, Chinese Academy of Sciences, Beijing 100080, People's Republic of China*

[2]*Department of Physics, China University of Mining & Technology, Beijing 100083, People's Republic of China*

(Received 17 May 2002; revised manuscript received 27 August 2002; published 28 January 2003)

A femtosecond laser driven collisional Ne-like Ti x-ray laser at 32.6 nm is numerically investigated using a hydrodynamic code coupled with an atomic data package for a 100-μm-thick Ti planar target irradiated by a single or double prepulse followed by an intense femtosecond laser pulse. By using an optimized drive pulse configuration, a gain of 40 cm^{-1} can be generated from a 5 mm$\times$50 μm line focus using only about 1 J pump energy.

DOI: 10.1103/PhysRevA.67.013810 PACS number(s): 42.55.Vc, 52.50.Jm, 52.59.Ye

I. INTRODUCTION

One of the main objectives in enhancing the efficiency of x-ray lasers is to develop ''table-top'' x-ray lasers for applications in university laboratories. In the ''traditional'' quasi-steady–state scheme, the prepulse is used only to create a preplasma. Delay is used to make a longer scale length. The main pulse then serves not only for heating the plasma to reach the electron temperature required by population inversion, but also for ionizing the plasma to the correct ionization state of Ne-like (Ni-like) ions [1,2]. By comparison, the prepulse and main pulse serve different functions in the transient collisional excitation (TCE) scheme. The prepulse is needed to prepare an optimized preplasma with a rich Ne-like (Ni-like) population. Then the main pulse heats the plasma rapidly to reach the required conditions with high electron temperature while keeping the ion temperature low. This is beneficial for forming a high gain in transient population inversion [3–10].

In this paper we numerically investigate the possibility of generating a Ne-like Ti x-ray laser from the $3p \rightarrow 3s$, $J=0 \rightarrow 1$ transition at 32.6 nm driven by femtosecond Ti:sapphire lasers, which are widely available at university laboratories. The pump geometry was set to be the standard line focus on a 100-μm-thick slab target. The one-dimensional (1D) Lagrangian hydrodynamic code MED103 [11] coupled with an atomic physics code and an atomic data package was used to predict the time evolution of laser-plasma interactions and to calculate the gain coefficient. The Ne-like Ti ion state was modeled for the ground state $2p^6$, all 26 excited levels of $2p^5 3s^1$, $2p^5 3p^1$, and $2p^5 3d^1$ states, and the next ionization stage (F-like states). The atomic physics code includes all possible radiative and collisional transitions between any two energy levels. Three different drive pulse configurations were studied: single prepulse, and double prepulse with short intervals (hundreds of picoseconds) and long intervals (nanoseconds). Detailed simulations were performed to optimize the drive pulse configurations.

*Author to whom correspondence should be addressed. Electronic address: jzhang@aphy.iphy.ac.cn

II. SIMULATIONS FOR SINGLE PREPULSE CONFIGURATION

The plasma modeling aims to find the optimum intensity and temporal delay between drive pulses. The prepulse was assumed to be from the chirped pulse before final compression. Such chirped pulses usually have durations of a few hundreds of picoseconds. The main pulse duration can be regulated from tens of femtosecond to a few picoseconds by changing the distance between the gratings in the compressor. In our simulations the durations of prepulse and main pulse were set to be 300 ps and 300 fs full width at half maximum, respectively. The main drive pulse of tens of femtoseconds duration is not suitable for collisional x-ray laser excitation because of its low energy absorption [12]. Both the prepulse and the main pulse have Gaussian profiles. The peak intensity of the main pulse at the line focus was fixed at 10^{15} W/cm^2.

It is well known that for ultrashort pulse driven collisional Ne-like x-ray lasers, the prepulse(s) should make the fraction of Ne-like ions in the preplasma as high as possible. We modeled the preplasma conditions produced by a single prepulse with different intensities. The optimum peak intensity of a 300 ps prepulse was found to be 3×10^{11} W/cm^2. Figure 1(a) shows the spatiotemporal profile of the ground state Ne-like ion fraction in the plasma produced by an optimized prepulse. The horizontal axis presents the spatial distance in the direction of plasma expansion. The initial position of the target surface is located at 100 μm. The prepulse reaches its peak at 720 ps on the time scale used in Fig. 1(a). The maximum fraction of the ground state Ne-like ions can be higher than 80%, but the high fraction region has a narrow spatial extent. From Fig. 1(a) we can also get the best starting time of the main pulse. Obviously, the main pulse should turn on in the time interval from 850 ps to 1 ns. The contours of the electron temperature and gain at 32.6 nm versus space and time for a 130 ps delay between prepulse and main pulse are shown in Fig. 1(b) and Fig. 1(c), respectively. We can see that the gain region has a small space-time extent, because after prepulse irradiation the preplasma is not well expanded. Figure 1(d) shows the spatial profile of the

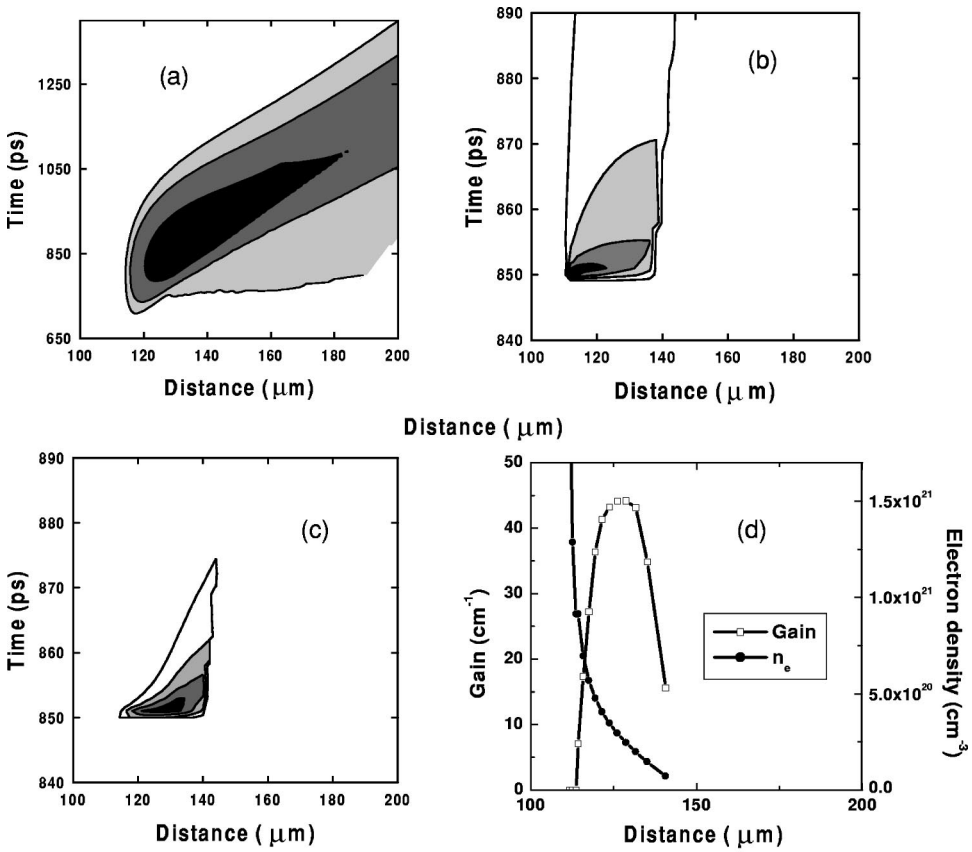

FIG. 1. (a) The ground state Ne-like Ti ion fraction versus space and time in the plasma generated by a 300 ps prepulse with a peak intensity of 3×10^{11} W/cm^2. The fraction in the plot is from 80% (black) to 40% (white) by steps of 20%. (b) Contours of electron temperature in the plasma after the main pulse irradiation. The temperature in the plot is from 400 eV (black) to 100 eV (white) by steps of 100 eV. (c) Contours of Ne-like Ti laser gain at 32.6 nm generated by a 300 fs main pulse. The gain in the plot is from 40 cm^{-1} (black) to 10 cm^{-1} (white) by steps of 10 cm^{-1}. (d) The spatial profiles of the local gain coefficient and electron density at the peak gain time.

local gain coefficient and electron density at the moment when the highest gain exists. The maximum local gain is 44 cm^{-1}. The critical density surface is located at 112 μm, where the electron density curve crosses the top frame of the figure. We can see that the gain region is located close to the critical density surface and has a high gradient of electron density. So this case is disadvantageous for the amplification of x-ray lasers.

III. DOUBLE PREPULSE WITH A SHORT INTERVAL

In order to improve the characteristics of the preplasma, a double prepulse configuration was considered. Earlier experiments showed that the double prepulse technique is an effective method to make a long scale and low density gradient preplasma [13]. In our simulations we used two 300 ps prepulses with 360 ps time delay. The first prepulse with 3×10^{11} W/cm^2 peak intensity can generate a Ne-like preplasma. The second prepulse is used to hold the ionization stage of the preplasma and give it more time to expand. This pulse configuration is equivalent to using a nanosecond prepulse followed by an ultrashort main pulse. The optimized peak intensity of the second prepulse was found to be 2×10^{11} W/cm^2. Figure 2(a) shows the much improved distribution of the ground state Ne-like ion fraction in the preplasma generated by such a double prepulse. Figures 2(b) and 2(c) show the electron temperature and gain generated by a 300 fs, 10^{15} W/cm^2 main pulse, which reaches its peak intensity 120 ps later than the second prepulse. The spatial profiles of the local gain coefficients and electron density at the time for the highest gain are given in Fig. 2(d). The maximum local gain was 40 cm^{-1}. From Fig. 2(d) we can see that the gain extent is about twice as wide as in the case of single prepulse pumping, and the density gradient in the gain region becomes much lower.

IV. DOUBLE PREPULSE WITH A LONG INTERVAL

A different drive configuration was also investigated with a double prepulse with a long delay. The time interval between two prepulses was increased up to 3 ns. A similar pump scheme was successfully used in some earlier x-ray laser experiments [14,15]. After 3 ns expansion, the ionization degree of the preplasma will fall due to the long cooling interval. The second prepulse with 5.3×10^{11} W/cm^2 peak intensity is used to ionize the preplasma to the Ne-like state again. The fraction of the ground state Ne-like ions in the plasma produced by this double prepulse is shown in Fig. 3(a). By irradiating the plasma with the 300 fs, 10^{15} W/cm^2 main pulse 300 ps later than the second prepulse, we obtained the electron temperature and gain contours shown in Figs. 3(b) and 3(c). The spatial profiles of the gain and the electron density at the peak gain time are shown in Fig. 3(d). For a longer interval between prepulses, the maximum gain

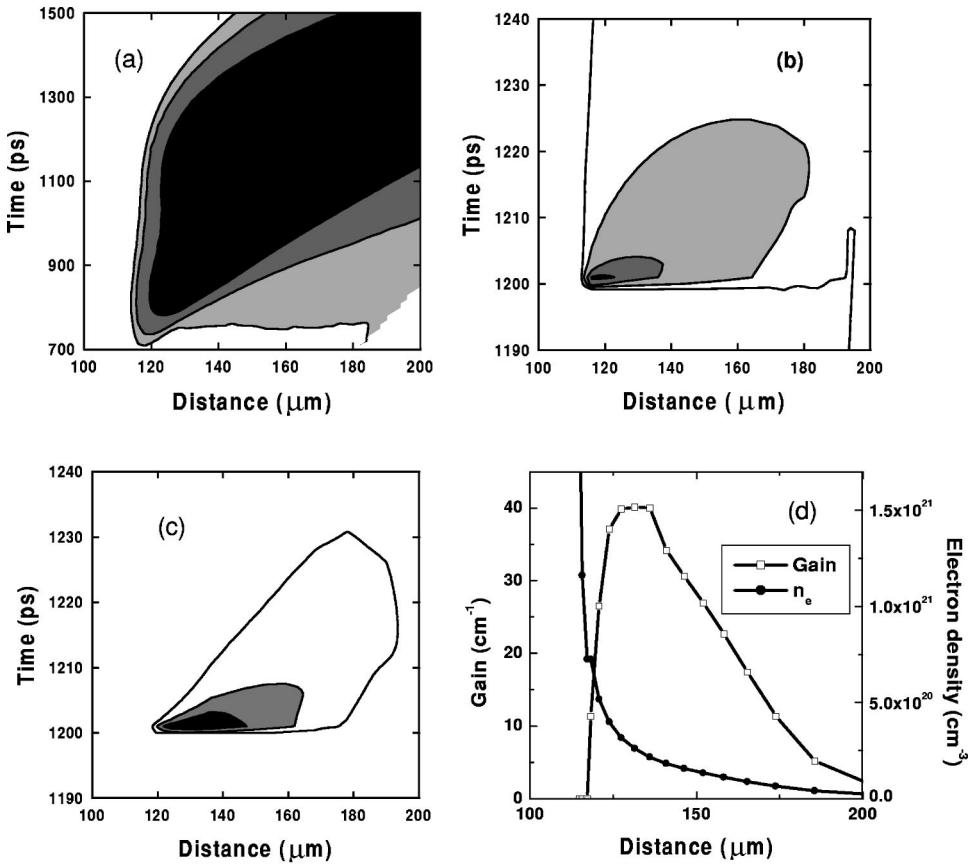

FIG. 2. (a) The ground state Ne-like Ti ion fraction versus space and time in the plasma generated by a double 300 ps prepulse with an interval of 360 ps. The fraction in the plot is from 80% (black) to 40% (white) by steps of 20%. (b) Contours of electron temperature in plasma after main pulse irradiation. The temperature in the plot is from 400 eV (black) to 100 eV (white) by steps of 100 eV. (c) Contours of Ne-like Ti laser gain at 32.6 nm generated by main pulse. The gain in the plot is from 30 cm^{-1} (black) to 10 cm^{-1} (white) by steps of 10 cm^{-1}. (d) The spatial profiles of the local gain coefficient and electron density at the peak gain time.

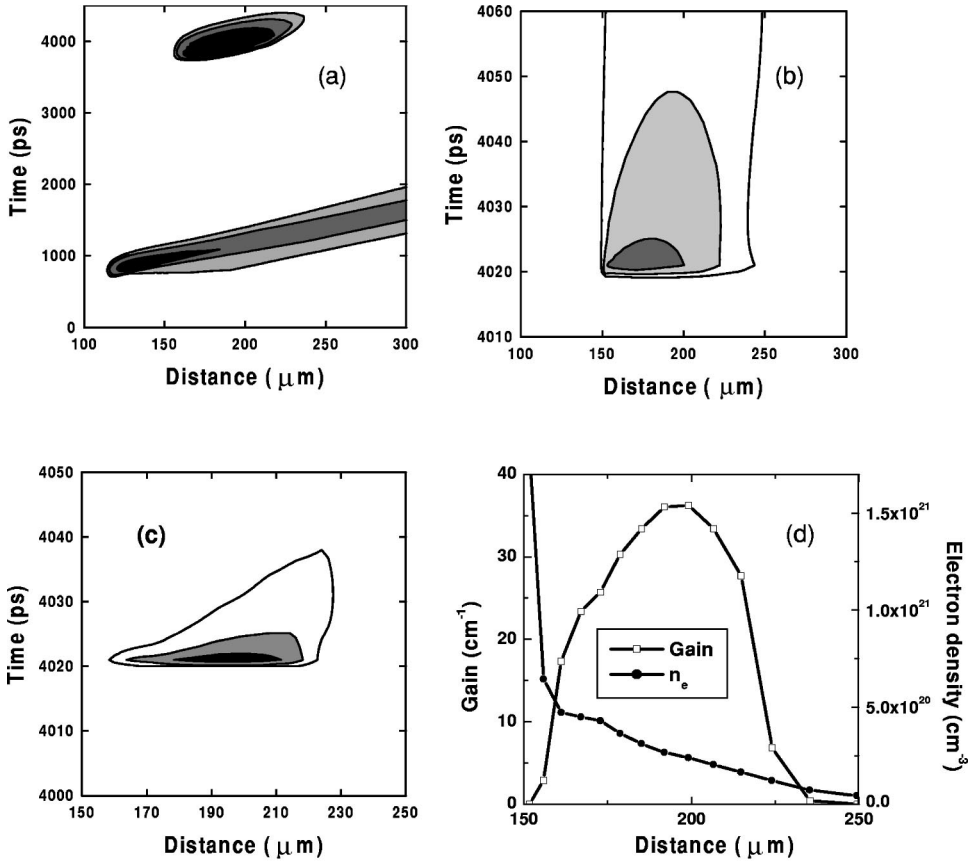

FIG. 3. (a) The ground state Ne-like Ti ion fraction versus space and time in the plasma generated by a double 300 ps prepulse with an interval of 3 ns. The fraction in the plot is from 80% (black) to 40% (white) by steps of 20%. (b) Contours of electron temperature in plasma after main pulse irradiation. The temperature in the plot is from 300 eV (black) to 100 eV (white) by steps of 100 eV. (c) Contours of Ne-like Ti laser gain at 32.6 nm generated by main pulse. The gain in the plot is from 30 cm^{-1} (black) to 10 cm^{-1}(white) by steps of 10 cm^{-1}. (d) The spatial profiles of the local gain coefficient and electron density at the peak gain time.

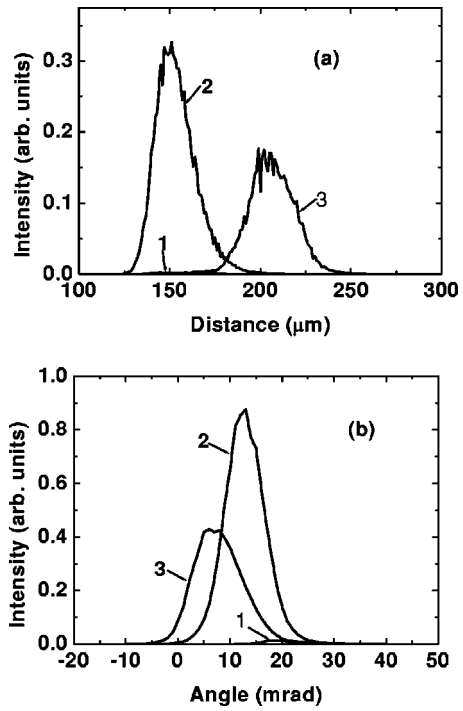

FIG. 4. The 32.6 nm x-ray laser output versus the source position (a) and the distribution angle (b) for single prepulse pumping (1), and double prepulse with short interval (2) and long interval (3).

falls to 36cm^{-1}, but the gain region has a broader spatial extent and lower density gradient.

In experiments, if we use a 5 mm$\times$50 μm line focus, the total pump energy for the three pump schemes described above will be 1 J, 1.2 J, and 1.4 J, respectively. We have also performed optimization for the Nd:glass laser wavelength using the same pump schemes; the gain coefficient is about twice as high. This situation is caused by the relatively long wavelength of the pump laser pulses, because the efficiency of the inverse bremsstralung absorption is inversely proportional to the square of the laser wavelength.

V. RAY TRACING CALCULATIONS

It is difficult to compare the efficiency of the pump schemes using a double prepulse with short and long delays only by looking at Fig. 2 and Fig. 3. In order to illustrate the role of refraction, we developed a 2D ray tracing postprocessor to calculate the relative output intensity of the x-ray laser for each pump scheme. The line focus was set to be 5 mm long. The plasma expansion during the short pulse pumping can be ignored. We assumed that traveling wave excitation is used, so the spatial profiles of gain and electron density can keep their form unchanged along the line focus. For simplification, the time evolution of the x-ray laser output was not included. In our ray tracing calculations the spatial profiles of gain and electron density are taken from Figs. 1(d), 2(d), and 3(d). Figure 4 shows the ray integrated output intensity of the 32.6 nm laser line in the near (a) and far (b) fields. The intensity of each ray is weighted by the upper-level population of the laser transition at the beginning of the ray. The result shows that the output intensity of single prepulse pumping is very small, and strong x-ray laser output can be obtained by using double prepulse schemes. When using a double prepulse with a short delay, the laser starts at 50 μm from the target surface and has $\sim$ 13 mrad tilt angle. When using a double prepulse with a long delay, the laser starts at 110 μm from the target surface and has $\sim$ 7 mrad tilt angle. Here we can see that using a double prepulse with long separation can really reduce the refraction, but the double prepulse with short delay produces the highest output intensity due to the relatively high gain coefficient. Altogether, the drive configuration of a double prepulse with a long delay does not have advantages in comparison with the case of a short delay beetween the prepulses. However, in some experiments with Ne-like Ge, the double prepulse with a long delay time was found to be a substantial improvement over a single nanosecond prepulse [14,15]. We believe that for ultrashort pulse pumping x-ray lasers, to use a double prepulse with a long delay is more effective for highly ionized ions like Ne-like Ge, Ni-like Sn, etc. But, for relatively low-ionized ions like Ne-like Ti or Ni-like Mo, the single nanosecond prepulse works best. The reason is that, in x-ray laser generation of highly ionized ions, most of the pump energy is spent on preparation of a properly ionized preplasma with a large scale length, using a double prepulse with a long delay can increase the efficiency of energy absorption of the prepulse, and finally save some total pump energy. X-ray lasers with low-ionized ions do not need much energy in the prepulse, so using a single nanosecond prepulse and a picosecond main pulse is a better choice.

VI. CONCLUSIONS

In conclusion, we have investigated a Ne-like Ti x-ray laser at 32.6 nm numerically using the one-dimensional hydrodynamic code MED103 coupled with an atomic data package for a 100-μm-thick Ti planar target irradiated by a single or double 300 ps prepulse followed by a 300 fs, 10^{15} W/cm^2 drive pulse from a Ti:sapphire laser. The optimization calculations were performed for various drive pulse combinations: single prepulse, and double prepulse with short (360 ps) and long (3 ns) intervals. The optimum intensity of the prepulse for each pump scheme was found. By using an optimized drive pulse configuration, an x-ray laser gain of about 40 cm^{-1} can be generated over a 5 mm$\times$50 μm line focus using a pump energy of only $\sim$ 1 J. We demonstrated the possibility of generating a Ne-like Ti soft x-ray laser at 32.6 nm using a table-top Ti:sapphire laser system. We also showed that the use of a double prepulse with a long delay time does not have any advantage for ultrashort pulse pumping of a Ne-like Ti x-ray laser.

ACKNOWLEDGMENTS

This work was supported by the National Nature Science Foundation of China under Grant Nos. 19974074, 19825110, and 60108007, and the National Hi-tech Program.

[1] J. Zhang, A. G. MacPhee, J. Nilsen, J. Lin, T. W. Barbee, Jr., C. Danson, M. H. Key, C. L. S. Lewis, D. Neely, R. M. N. O'Rourke, G. J. Pert, R. Smith, G. J. Tallents, J. S. Wark, and E. Wolfrum, Phys. Rev. Lett. **78**, 3856 (1997).

[2] J. Zhang, A. G. MacPhee, J. Lin, E. Wolfrum, R. Smith, C. Danson, M. H. Key, C. L. S. Lewis, D. Neely, J. Nilsen, G. J. Pert, G. J. Tallents, and J. S. Wark, Science **276**, 1097 (1997).

[3] P. V. Nickles, V. N. Shlyaptsev, M. Kalachnikov, M. Schnürer, I. Will, and W. Sandner, Phys. Rev. Lett. **78**, 2748 (1997).

[4] J. Dunn, A. L. Osterheld, R. Shepherd, W. E. White, V. N. Shlyaptsev, and R. E. Stewart, Phys. Rev. Lett. **80**, 2825 (1998); J. Dunn, J. Nilsen, A. L. Osterheld, Y. Li, and V. N. Shlyaptsev, Opt. Lett. **24**, 101 (1999).

[5] M. P. Kalachnikov, P. V. Nickles, M. Schnürer, W. Sandner, V. N. Shlyaptsev, C. Danson, D. Neely, E. Wolfrum, J. Zhang, A. Behjat, A. Demir, G. J. Tallents, P. J. Warwick, and C. L. S. Lewis, Phys. Rev. A **57**, 4778 (1998).

[6] J. Nilsen, Y. L. Li, and J. Dunn, J. Opt. Soc. Am. B **17**, 1084 (2000).

[7] Y. J. Li and J. Zhang, Phys. Rev. E **63**, 036410 (2001); Y. J. Li, X. Lu, and J. Zhang, *ibid.* **66**, 046501 (2002).

[8] J. Nilsen, B. J. MacGowan, L. B. Da Silva, and J. C. Moreno, Phys. Rev. A **48**, 4682 (1993).

[9] Y. L. Li, J. Dunn, J. Nilsen, T. W. Barbee, Jr., A. L. Osterheld, and V. N. Shlyaptsev, J. Opt. Soc. Am. B **17**, 1098 (2000).

[10] J. Dunn, Y. Li, A. L. Osterheld, J. Nilsen, J. R. Hunter, and V. N. Shlyaptsev, Phys. Rev. Lett. **84**, 4834 (2000).

[11] J. P. Christiansen, D. E. T. F. Ashby, and K. V. Roberts, Comput. Phys. Commun. **7**, 271 (1974).

[12] X. Lu, Y. J. Li, and J. Zhang, Phys. Plasmas **9**, 1412 (2002).

[13] F. Löwenthal, R. Tommasini, and J. E. Balmer, Opt. Commun. **154**, 325 (1998); J. E. Balmer, R. Tommasini, and F. Löwenthal, IEEE J. Sel. Top. Quantum Electron. **5**, 1435 (1999).

[14] J. Y. Lin, G. J. Tallents, A. G. MacPhee, A. Demir, C. L. S. Lewis, R. M. N. O'Rourke, G. J. Pert, D. Ros, and P. Zeitoun, Opt. Commun. **166**, 211 (1999).

[15] R. E. King, G. J. Pert, S. P. McCabe, P. A. Simms, A. G. MacPhee, C. L. S. Lewis, R. Keenan, R. M. N. O'Rourke, G. J. Tallents, S. J. Pestehe, F. Strati, D. Neely, and R. Allott, Phys. Rev. A **64**, 053810 (2001).